

Muon anomalous magnetic moment and Right handed sterile neutrino

Iman Motie,^{1,*} S. Mahmoudi,^{2,†} Mahdi Sadegh,^{3,‡} Jafar
Khodagholizadeh,^{4,§} Alain Blanchard,^{1,¶} and S.-S. Xue^{5,||}

¹*Université de Toulouse, UPS-OMP, IRAP, F-31400 Toulouse, France,
CNRS, IRAP, 14 avenue Edouard Belin, F-31400 Toulouse, France*

²*Department of Physics, School of Science, Shiraz University, Shiraz 71454, Iran*

³*School of Particles and Accelerators, Institute for Research in
Fundamental Sciences (IPM), P. O. Box 19395-5531, Tehran, Iran*

⁴*Farhangian University, P.O. Box 11876-13311, Tehran, Iran*

⁵*ICRANet Piazzale della Repubblica, 10 -65122, Pescara, Italy,
Physics Department, Sapienza University of Rome, Rome, Italy,
INFN, Sezione di Perugia, Perugia, Italy,*

ICTP-AP, University of Chinese Academy of Sciences, Beijing, China.

The muon's magnetic moment is a fundamental quantity in particle physics and the deviation of its value from quantum electrodynamics (QED), motivates research beyond the standard models (SM). In this study, we utilize the effective coupling of right-handed sterile neutrinos with SM gauge bosons to calculate the muon anomalous magnetic moment (μ AMM) at one-loop level. The contribution of the sterile neutrino interactions on the μ AMM is calculated by considering the standard and non-standard neutrino interactions. Our results show that the standard sterile neutrino interactions give a negligible contribution to Δa_μ while the non-standard neutrino interactions can play a significant role in explaining the muon ($g - 2$) anomaly. In the context of the non-standard neutrino interaction, our calculation shows that a Dirac mass scale M_D around 100 GeV could explain the muon anomaly if the right handed sterile neutrino's coupling with SM particles is about $\mathcal{G}_R \approx 10^{-3}$. We have also plotted the allowed region of the model parameters that satisfy the experimental data on Δa_μ^{SN} and discuss the percentage of the μ anomaly compensation in terms of the coupling constant \mathcal{G}_R .

* iman.motie@univ-tlse3.fr

† s.mahmoudi@shirazu.ac.ir

‡ m.sadegh@ipm.ir

§ gholizadeh@ipm.ir

¶ alain.blanchard@irap.omp.eu

|| xue@icra.it

I. INTRODUCTION

Over the past decades, despite the great success of the SM of particle physics, it still challenged by some experimental anomalies, such as dark matter (DM) relic density [1, 2], mass of neutrinos [3], and baryon asymmetry of the Universe [4].

Another long-standing anomaly is related to the μ AMM, $a_\mu \equiv (g-2)_\mu/2$. More recently, it has been reported a new measurement of a_μ using data collected in 2019 (Run-2) and 2020 (Run-3) by the Muon $(g-2)$ Experiment at Fermi National Accelerator Laboratory (FNAL) [5] as well as the Brookhaven National Laboratory (BNL) [6]

$$\begin{cases} a_\mu^{\text{FNAL}} = (116\,592\,055 \pm 24) \times 10^{-11} \\ a_\mu^{\text{BNL}} = (116\,592\,089 \pm 63) \times 10^{-11} \end{cases} \quad (1)$$

leading to the combined (BNL and FNAL) experimental average [5]

$$a_\mu^{\text{exp}} = (116\,592\,059 \pm 22) \times 10^{-11}, \quad (2)$$

which differs from the SM theory prediction [7]

$$a_\mu^{\text{SM}} = (116\,591\,810 \pm 43) \times 10^{-11}. \quad (3)$$

The above results represent that the SM prediction is more than 5σ smaller than the latest experimental measurement

$$\Delta a_\mu = a_\mu^{\text{exp}} - a_\mu^{\text{SM}} = (2.49 \pm 0.48) \times 10^{-9}. \quad (4)$$

Although such a discrepancy makes the importance of clarifying the correct SM theoretical calculation significant [8], it has generated great interest in the particle physics community because if the current anomaly is confirmed, it can probably be considered to be strong evidence of new physics beyond the SM and might arise from the effects of as-yet-undiscovered particles contributing through virtual loops.

From the theoretical point of view, a large number of researches have been done to investigate the problem of muon anomalous magnetic dipole moment in various scenarios; More recent lattice QCD results attempt to explain μ AMM inside the SM using leading hadronic contribution [8]. Moreover, there have already been a great number of theoretical works trying to explain this anomaly by new physics [9–23]. One of the most important classes of these theories focuses on new

physics including sterile neutrinos. For instance, the μ AMM has been discussed within the context of a model based on the $SU_L(2) \times SU_R(2) \times U(1)_{B-L}$ -gauge group in [24]. Moreover, authors in [25] have considered a gauged $U(1)_{L_\mu-L_\tau}$ extension of the left-right symmetric theory in order to simultaneously explain neutrino mass, mixing and the μ AMM. In addition, this anomaly has been address through models with mirror symmetry and type I see-saw mechanism at low energy scale of electroweak interactions in [26]. Furthermore, Abdallah et al. in [27] have analyzed the μ AMM in TeV scale $B - L$ extension of the SM with inverse seesaw mechanism.

In this work, we continue the investigation of the muon anomaly in the context of an effective model based on the fundamental symmetries and particle content of the SM [28–30]. This scenario was motivated by the parity symmetry reconstruction at high energies without any extra gauge bosons and introduces three massive sterile neutrinos ν_R as well as the SM gauge symmetric four-fermion interactions giving rise to new effective interactions between sterile neutrinos and SM gauge bosons. We will study the interaction effects of this sort of sterile neutrino with SM particles on the μ AMM.

This paper is organized as follows. A brief review of the theoretical aspects of the $g - 2$ has been provided in Section II. In Section III, we review the sterile neutrino's effective lagrangian and its interaction with gauge bosons. Section IV is devoted to the calculation of the sterile neutrino corrections to μ AMM: In subsection IV A, we study the contribution due to W boson and ν_R mediation (standard interaction) and the contribution arising from W boson mediation with Left-Right neutrino mixing (non-standard interaction) is discussed in subsection IV B. In Section V, we give some concluding remarks. Finally, the detail of calculations of the sterile neutrino corrections to a_μ has been presented in Appendix A.

II. ELECTROMAGNETIC FORM FACTORS AND μ AMM

According to quantum mechanics, any elementary charged particle with intrinsic angular momentum (\vec{s}) has a magnetic dipole moment ($\vec{\mu}$) which is related to its spin through the following equation,

$$\vec{\mu} = g \left(\frac{q}{2m} \right) \vec{s}, \quad (5)$$

where $q = \pm e$ is the electric charge of a given charged particle and m denotes its mass. In addition, g indicates the gyromagnetic ratio which is equal to 2 in classical quantum mechanics. However, the calculations of the loop corrections in quantum field theories, like the SM, show that this quantity

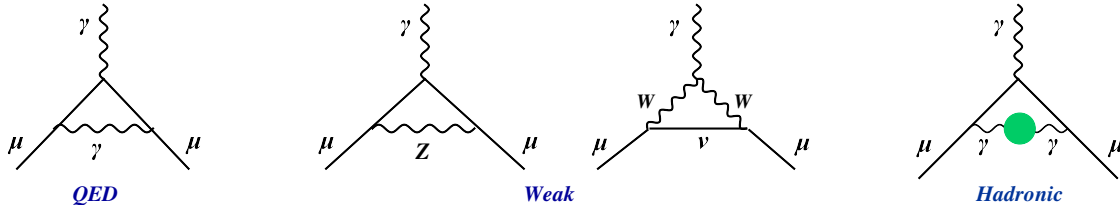


FIG. 1. Lowest-order SM corrections to a_μ . From left to right: QED, weak, and hadronic [13].

receives contributions from radiative corrections. Indeed, since the interaction of the elementary particle with a photon is modified by additional interactions with virtual particles, the value of g is modified, resulting in increasing its value from the tree-level prediction of $g = 2$. For the charged lepton ($l = e, \mu, \tau$), these corrections are parametrized in terms of a_l which is defined as the fractional deviation from the quantum classical prediction of $g_l = 2$ as follows

$$a_l = (g - 2)_l/2, \quad (6)$$

referred to as the anomalous magnetic moment. This quantity is a special one that has continued to serve as a long-standing test of the SM. Up to now, a great deal of effort has been put forth to determine the SM modifications to g from virtual SM particles up to a sufficient order [7, 8, 31–36]. Comparison between the theoretical and experimental measurements of a_l leads to the studies of lepton magnetic moments which is a powerful indirect probe for new physics.

Regarding the muon particle, there exists a deviation between the prediction of the SM and the most precise measurement performed [5, 7]. Additionally, the experimental value of a_μ cannot be explained solely by the SM, and one must take into account not only the loop corrections through the SM framework but also the contribution from new physics (NP) beyond the SM [16, 37, 38].

$$a_\mu = a_\mu^{SM} + a_\mu^{NP}, \quad (7)$$

where a_μ^{NP} contains all effects on the anomalous magnetic moment of the muon from physics beyond the SM and

$$a_\mu^{SM} = a_\mu^{QED} + a_\mu^{Weak} + a_\mu^{hadron}, \quad (8)$$

where the a_μ^{QED} includes the Schwinger result [39, 40] plus corrections up to five loops, a_μ^{Weak} shows the weak contribution with the loops containing the heavy bosons W^\pm , Z , and H and the hadronic part a_μ^{hadron} shows the contribution of hadrons in the loop corrections[7]. The corresponding Feynman diagrams are depicted in Fig. 1.

In quantum electrodynamics (QED), loop effects in the electromagnetic interaction of fermionic point particles are typically studied using electromagnetic form factors to parameterize currents. The vector current is a Lorentz vector that can be expanded in terms of all independent Lorentz vectors in the system being considered. This means that the most general form for the electromagnetic current between Dirac leptons, satisfying Lorentz covariance and the Ward identity, can be expressed as follows

$$\langle \psi(p) | J_\mu^{EM} | \psi(p') \rangle = \bar{u}(p') \mathcal{F}_\mu(q^2) u(p), \quad (9)$$

where $q_\mu = p'_\mu - p_\mu$ and

$$\mathcal{F}_\mu(q^2) = F_1 \gamma_\mu + F_2 i \frac{\sigma_{\mu\nu} q^\nu}{2m} + F_3 (q_\mu - \frac{q^2}{2m} \gamma_\mu) \gamma_5 + F_4 \sigma_{\mu\nu} \frac{q^\nu}{2m} \gamma_5, \quad (10)$$

in which, m stands for the mass of the charged lepton (specifically the muon), while F_i 's with i ranging from 1 to 4 represent the standard electric charge, magnetic dipole, anapole (axial charge), and electric dipole form factors, respectively. In this study, we focus solely on F_2 for muon and compute its corrections from the right handed sterile neutrinos' contribution in the following sections.

III. STERILE NEUTRINOS INTERACTIONS WITH SM PARTICLES

Sterile neutrinos are a type of hypothetical particle that can potentially elucidate various inexplicable phenomena observed in particle physics experiments. For instance, they could play a significant role in unraveling the mystery surrounding DM [41–43]. Sterile neutrinos could also offer a natural explanation for the small active neutrino masses implied by neutrino oscillation [44].

The idea of right-handed neutrinos, known as sterile neutrinos, is highly plausible as all other fermions have been observed with both left and right chirality, while active neutrinos have only been detected in a left-handed state. Moreover, they could provide a natural explanation for the tiny active neutrino masses deduced from neutrino oscillation [45]. Assuming sterile neutrinos exist, there must be a minimum of three types present to support the ideas of leptogenesis and DM. This requirement is in contrast to the necessity of having exactly three active neutrino types for ensuring the electroweak interaction is free from anomalies [46].

Here, we briefly describe the ultraviolet (UV) completion of the low-energy effective model adopted in this work. On one hand, as shown in low-energy experiments, the SM possesses parity-violating (chiral) gauge symmetries $SU_c(3) \times SU_L(2) \times U_Y(1)$. On the other hand, as a well-defined

quantum field theory, the SM should regularize at the high-energy cutoff Λ_{cut} , fully preserving the SM gauge symmetries. A natural UV regularization is provided by a theory of new physics at Λ_{cut} , for instance, quantum gravity. However, The natural UV regularization and the bilinear fermion Lagrangian of SM chiral gauge symmetries have a theoretical inconsistency due to the No-Go theorem [47, 48]. This inconsistency suggests the existence of right-handed neutrinos and their quadrilinear four-fermion operators at the UV cutoff scale Λ_{cut} . Therefore, we adopt the four-fermion operators of the torsion-free Einstein-Cartan Lagrangian with SM leptons ψ^f and three right-handed sterile neutrinos ν_R^f [28, 29]:

$$\mathcal{L} \supset -G_{\text{cut}} \sum_{l=1,2,3} \left(\bar{\nu}_R^{lc} \nu_R^l \bar{\nu}_R^l \nu_R^{lc} + \bar{\nu}_R^{lc} \psi_R^l \bar{\psi}_R^l \nu_R^{lc} \right) + \text{h.c.}, \quad (11)$$

where $G_{\text{cut}} \propto \Lambda_{\text{cut}}^2$ and the two-component Weyl fermions ν_R^l and ψ_R^l respectively are the eigenstates of the SM gauge symmetries. The effective four-fermion operators (11) are relevant to the topic studied in this article. We do not consider other types of four-fermion operators in Ref. [29, 30]. These operators possess (i) a strong coupling phase where composite particles are formed and symmetries are preserved, (ii) a weak coupling phase where spontaneous symmetry breaking occurs and elementary particles acquire masses. The details are given in Refs. [29, 30] and [49]. In this paper, we will consider the second possibility, i.e. the symmetry breaking phase.

In the four-fermion interactions (11), the neutrino self-interaction undergoes spontaneous symmetry breaking to generate the Majorana masses $M_M^l = -G_{\text{cut}} \langle \bar{\nu}_R^{lc} \nu_R^l \rangle$. It is accompanied by a Goldstone boson (Axion or Majoron) and a massive scalar χ -boson. The properties and observational consequences of these are discussed in Ref. [50]. The neutrino Dirac masses M_D^l are generated by usual Yukawa interactions involving the Higgs field, right-handed neutrinos and left-handed leptons. Therefore, neutrino mass terms consist of the Majorana mass M_M^l and Dirac mass M_D^l ,

$$M_M^l \bar{\nu}_R^{lc} \nu_R^l + M_D^l \bar{\nu}_L^l \nu_R^l + \text{h.c.} \quad (12)$$

Here, we suppose that M_M^l and M_D^l are free parameters and $M_M^l \gg M_D^l$ [29]. Via the sea-saw mechanism, three Majorana active neutrinos ($\nu_L^l + \nu_L^{lc}$) masses are given by $M_{\nu_i} \approx (M_D^l)^2 / (4M_M^l)$. Three Majorana sterile neutrinos ($\nu_R^l + \nu_R^{lc}$) masses are given by $M_{N_i} \approx M_M^l$.

On the other hand, the second four-fermion operator in (11) shows neutrinos' interactions with SM charged leptons ψ_R^l . These effectively *induce* in low energies the one-particle-irreducible (1PI)

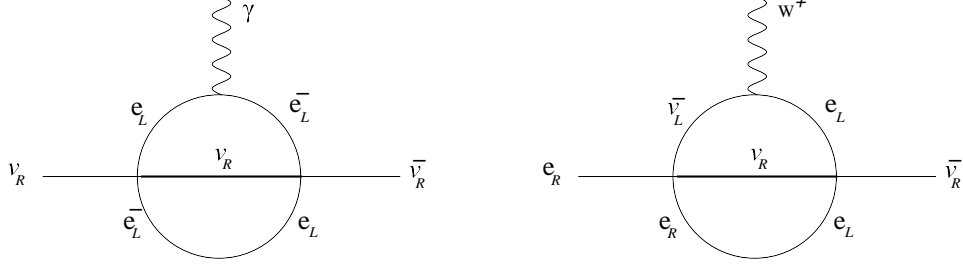


FIG. 2. The possible sunset diagrams from the second term of (11), namely, sterile neutrino and SM fermion four-fermion interactions $\bar{\nu}_R^{fc} \psi_R^f \bar{\psi}_R^f \nu_R^{fc}$, in which ψ_R^f represents SM right-handed fermions. Hence, these 1PI vertexes lead to effective SM gauge boson couplings to right-handed neutrinos (13). Left: the effective 1PI interacting vertex (13) of the gauge boson W^+ and right-handed sterile neutrino ν_R^ℓ , for more details see Figure 3 of Ref. [51]. Right: the effective 1PI interacting vertex (13) of photon γ and right-handed sterile neutrino ν_R^ℓ , and similar one for Z^0 boson. The slightly thick solid lines inside sunset diagrams represent right-handed neutrino propagators with Dirac mass (left) or Majorana mass (right). A Dirac mass term is present in the internal electron propagator from e_L to e_R in the left sunset diagram. [50].

vertexes [50]

$$\begin{aligned} \mathcal{L} \supset & \mathcal{G}_R^W (g_w/\sqrt{2}) \bar{\ell}_R \gamma^\mu \nu_R^\ell W_\mu^- + \mathcal{G}_R^Z (g_w/\sqrt{2}) \bar{\nu}_R^\ell \gamma^\mu \nu_R^\ell Z_\mu^0 \\ & + \mathcal{G}_R^\gamma (e) \bar{\nu}_R^\ell \gamma^\mu \nu_R^\ell A_\mu + \text{h.c.} \end{aligned} \quad (13)$$

of right-handed currents interacting with the SM gauge bosons.

It is important to note that the four-fermion interaction of only right-handed sterile neutrinos in the Lagrangian (11) does not induce the effective right-handed coupling of the W boson. Essentially, the four-fermion interactions introduce a small mixing between right-handed neutrinos and left-handed leptons, leading to an effective W boson coupling to right-handed currents. To be more clear, we have provided Fig. 2 in which the sun-set Feynman diagrams depict the 1PI interacting vertexes, showing that these vertexes can be effectively induced from the second four-fermion operator of Eq. (11). This reveals that right-handed neutrinos interact with SM leptons. In other words, the four-fermion interactions introduce the small mixing between right-handed neutrinos and left-handed leptons, leading to an effective coupling of W and right-handed current ¹. The effective couplings $\mathcal{G}_R^{W,Z,\gamma}$ are energy-dependent functions and are generally small at low energies. In this paper, we treat them as effective parameters. Moreover, it is worth mentioning that the resulting Axion or Majoron in the model has a small coupling to SM particles, which is linked to

¹The four-fermion interaction of only right-handed sterile neutrinos in the Lagrangian (11) does not induce the effective right-handed coupling of W boson.

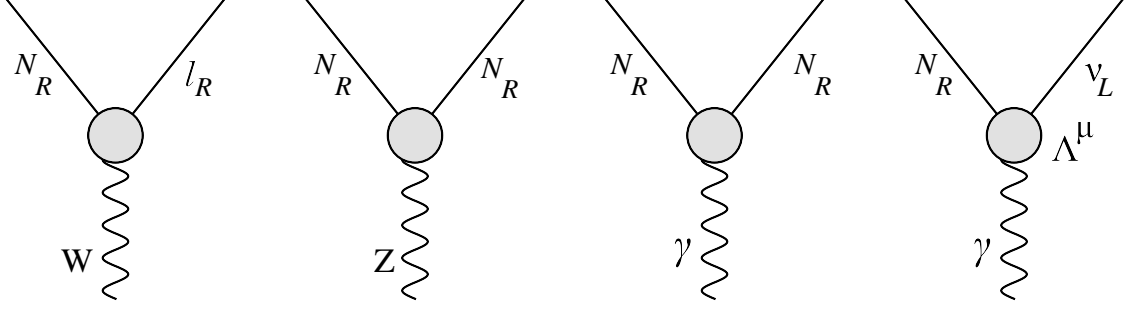


FIG. 3. The effective coupling of right-handed current with W , Z bosons and photon, which are not present in the SM. The corresponding expressions are Eqs. (14) and (15).

the smallness of the effective right-handed coupling \mathcal{G}_R , rather than heavy sterile neutrino masses (see Ref. [50] for detailed discussions and calculations).

Moreover, we present the Feynman diagrams corresponding to these possible interaction vertexes in Fig. 3. Two left Feynman diagrams correspond to the interaction of the sterile neutrino with W and Z bosons based on the Eq. (13), and sterile neutrino-photon vertexes in (13) are shown in two right diagrams. The charged current interacts with W^\pm gauge boson and the neutral currents interact with A^μ photon and Z_μ boson. The SM gauge couplings $g_w = e/\sin\theta_W$, the electric charge e and Weinberg angle θ_W relate to the Fermi constant as $G_F/\sqrt{2} = g_w^2/8M_W^2$. The effective right-handed couplings \mathcal{G}_R^W , \mathcal{G}_R^Z and \mathcal{G}_R^γ are small dimensionless parameters beyond the SM. Their upper limits must be constrained by Earth-based experiments and astrophysical and cosmological observations. We assume they are in the same order and adopt unique notation $\mathcal{G}_R \ll 1$.

The right-handed neutrino ν_R^ℓ is in the same family of the charged lepton $\bar{\ell}_R$. The right-handed doublets (ν_R^ℓ, ℓ_R) are gauge eigenstates, and (N_R^ℓ, ℓ_R) are the corresponding mass eigenstates. In terms of mass eigenstates (N_R^ℓ, ℓ_R) , gauge eigenstates $\nu_R^\ell = (U_R^\nu)^{\ell\ell'} N_R^{\ell'}$ and $\ell_R = (U_R^\ell)^{\ell\ell'} \ell_R^{\ell'}$, where U_R^ν and U_R^ℓ are 3×3 unitary matrices in family flavor space, the 1PI interactions (13) take the following form

$$\begin{aligned} \mathcal{L} \supset & \mathcal{G}_R^W (g_w/\sqrt{2}) [(U_R^\ell)^\dagger U_R^{\nu\ell}] \bar{\ell}_R \gamma^\mu N_R^\ell W_\mu^- + \mathcal{G}_R^Z (g_w/\sqrt{2}) \bar{\nu}_R^\ell \gamma^\mu \nu_R^\ell Z_\mu^0 \\ & + \mathcal{G}_R^\gamma (e) \bar{\nu}_R^\ell \gamma^\mu \nu_R^\ell A_\mu + \text{h.c.} \end{aligned} \quad (14)$$

where the flavor mixing matrix $V_R^{\ell\ell'} = [(U_R^\ell)^\dagger U_R^{\nu\ell'}]$ appears in charged current interaction, while neutral current one remains diagonal in lepton family flavor space [28]. Note that the $V_R^{\ell\ell'}$ differs from the Pontecorvo-Maki-Nakagawa-Sakata (PMNS) one $V_L^{\ell\ell'} = [(U_L^\ell)^\dagger U_L^{\nu\ell'}]$, which associates to the SM left-handed current interaction $\bar{\nu}_L^\ell \gamma^\mu \ell_L^\ell W_\mu^-$. Summation over three lepton families is

performed in Eq. (14) and no flavor-changing-neutral-current (FCNC) interactions occur.

The effective operator \mathcal{G}_R^W contributes to vector boson fusion (VBF) processes, see the left Feynman diagram in Fig. 1 of Ref. [52]. Moreover, the constraints on the sterile neutrinos' mixing $|V_R|$ and masses M_{N^ℓ} have been studied [52–54], indicating that the upper limit of \mathcal{G}_R value should be smaller than 10^{-4} . It is constrained by studying the ratio of top- and bottom-quark masses [55], the double beta-decay $0\nu\beta\beta$ experiment [56], W^\pm and Z^0 decay widths [57], W boson mass tension [58], CMB cosmic birefringence [59], and the precision measurement of fine-structure constant α [50].

Regarding N_R^e as a DM particle in the XENON1T experiment and astrophysical observations [60], one studied the relevant 1PI vertex $[(U_L^\nu)^\dagger U_L^\ell]^{ll'} \bar{\nu}_L^l \Lambda_{l'}^\mu \nu_R^{l'} A_\mu$,

$$\Lambda_{l'}^\mu(q) = i \frac{eg_w^2 \mathcal{G}_R m_{l'}}{16\pi^2} \left[(C_0 + 2C_1) p_1^\mu + (C_0 + 2C_2) k_1^\mu \right] \quad (15)$$

which is induced by the effective Lagrangian (13). Depicted by the last Feynman diagram in Fig. 3, this 1PI vertex $\Lambda_{l'}^\mu$ belongs to the effective interacting Lagrangian (14) of the leading order \mathcal{G}_R . Here p_1^μ and k_1^μ represent the four-momenta of incoming sterile neutrinos and outgoing SM neutrinos, respectively. The three-point Passarino-Veltman functions [61] C_0 , C_1 and C_2 approach M_W^{-2} in the zero momentum transfer limit $q^2 = (k_1 - p_1)^2 \rightarrow 0$. Among possible induced 1PI operators in low energies, we study in this article relevant ones possibly accounting for the Muon a_μ anomaly.

IV. PREDICTION ON THE μ AMM

In this section, we aim to calculate the magnetic dipole form factor (F_2) for the muon particle while considering the contributions of the right-handed sterile neutrinos using the effective 1PI operators (14) and (15).

A. Contribution due to W boson and ν_R mediation: Standard neutrino interactions

To this end, we first need to sketch all feasible one-loop Feynman diagrams which include W boson and ν_R mediation. In our case, there are three novel vertex corrections shown in Fig. (4), where below, you can find the vertex correction for each of these three diagrams (a), (b) and (c):

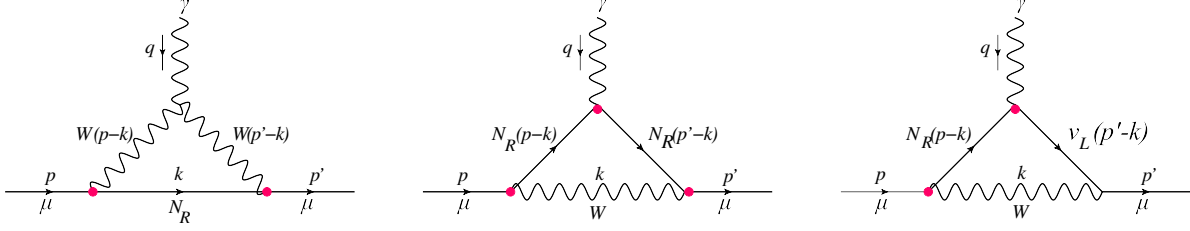


FIG. 4. The contributions of sterile neutrinos ν_R , SM (Active) neutrinos ν_L and W bosons to the one-loop vertex correction of the muon anomalous magnetic moment. The red spots indicate the effective interacting vertices depicted in Fig. 3, which are absent in the SM.

$$\begin{aligned}
\bar{u}(p') \left(-ie\Gamma_{(a)}^\mu \right) u(p) &= -ie V_R^{\mu l} V_R^{\dagger \mu l} \int \frac{d^4 k}{(2\pi)^4} \\
&\times \left\{ \bar{u}(p') \left(\frac{-i\mathcal{G}_R g_w}{2\sqrt{2}} \right) \gamma^\nu (1 + \gamma_5) \frac{i}{\not{k} - M_{N_l}} \left(\frac{-i\mathcal{G}_R g_w}{2\sqrt{2}} \right) \gamma^\rho (1 + \gamma_5) \right. \\
&\times u(p) \frac{-i}{(p-k)^2 - M_W^2} \frac{-i}{(p'-k)^2 - M_W^2} \left[g_{\rho\alpha} - \frac{(p-k)_\rho (p-k)_\alpha}{M_W^2} \right] \\
&\times \left[g_{\nu\beta} - \frac{(p'-k)_\nu (p'-k)_\beta}{M_W^2} \right] \left[g^{\beta\alpha} (2k - p - p')^\mu \right. \\
&\left. \left. + g^{\alpha\mu} (2p - p' - k)^\beta + g^{\mu\beta} (2p' - k - p)^\alpha \right] \right\}, \quad (16)
\end{aligned}$$

$$\begin{aligned}
\bar{u}(p') \left(-ie\Gamma_{(b)}^\mu \right) u(p) &= -ie V_R^{\mu l} V_R^{\dagger \mu l} \int \frac{d^4 k}{(2\pi)^4} \\
&\times \left\{ \bar{u}(p') \left(\frac{-i\mathcal{G}_R g_w}{2\sqrt{2}} \right) \gamma^\nu (1 + \gamma_5) \frac{i}{\not{p}' - \not{k} - M_{N_l}} i\mathcal{G}_R^\gamma \gamma^\mu (1 + \gamma_5) \right. \\
&\times \left. \frac{i}{\not{p} - \not{k} - M_{N_l}} \left(\frac{-i\mathcal{G}_R g_w}{2\sqrt{2}} \right) \gamma^\rho (1 + \gamma_5) u(p) \frac{-i}{k^2 - M_W^2} \left[g_{\rho\nu} - \frac{k_\rho k_\nu}{M_W^2} \right] \right\} \quad (17)
\end{aligned}$$

$$\begin{aligned}
\bar{u}(p') \left(-ie\Gamma_{(c)}^\mu \right) u(p) &= -ie V_R^{\mu l} \int \frac{d^4 k}{(2\pi)^4} \\
&\times \left\{ \bar{u}(p') \left(\frac{-ig_w}{2\sqrt{2}} \right) \gamma^\nu (1 - \gamma_5) \frac{i}{\not{p}' - \not{k} - M_{N_l}} i \left(\frac{-\mathcal{G}_R g_w^2 m_l}{16\pi^2} \right) \right. \\
&\times \left((C_0 + 2C_1)(p' - k)^\mu + (C_0 + 2C_2)(p - k)^\mu \right) \frac{i}{\not{p} - \not{k} - M_{\nu_l}} \\
&\times \left. \left(\frac{-i\mathcal{G}_R g_w}{2\sqrt{2}} \right) \gamma^\rho (1 + \gamma_5) u(p) \frac{-i}{k^2 - M_W^2} \left[g_{\rho\nu} - \frac{k_\rho k_\nu}{M_W^2} \right] \right\}, \quad (18)
\end{aligned}$$

in which $u(p)$ is the ordinary free Dirac spinor, M_W , M_N , and M_ν are the masses of the W boson, sterile neutrino, and SM left-handed neutrino, respectively. Indices (a), (b), and (c) on the left-hand side pertain to the Feynman diagrams depicted in Fig.(4). After performing straightforward computations at zero momentum transfer ($q^2 \rightarrow 0$) and singling out the part to be proportional

to $(p + p')^\mu$, the contribution made by the right handed sterile neutrino into the μ AMM will be obtained as follows

$$\begin{aligned} \Delta a_\mu^{SN(a)} &= 2 \left(\frac{\mathcal{G}_R g_w}{4\pi} \right)^2 m_\mu^2 V_R^{\mu l} V_R^{\dagger \mu l} \int_0^1 dz \int_0^{1-z} dy \\ &\quad \times \frac{2y + 4yz + 4z^2}{(y+z)M_W^2 + (1-y-z)M_{N_l}^2 - (y+z)(1-y-z)m_\mu^2}. \end{aligned} \quad (19)$$

$$\begin{aligned} \Delta a_\mu^{SN(b)} &= - \left(\frac{\mathcal{G}_R g_w}{\pi} \right)^2 \mathcal{G}_R^\gamma m_\mu^2 V_R^{\mu l} V_R^{\dagger \mu l} \int_0^1 dz \int_0^{1-z} dy \\ &\quad \times \frac{-1 + 2z + y - yz - z^2}{(y+z)M_{N_l}^2 + (1-y-z)M_W^2 - (y+z)(1-y-z)m_\mu^2}. \end{aligned} \quad (20)$$

$$\begin{aligned} \Delta a_\mu^{SN(c)} &= \frac{\mathcal{G}_R^2 g_w^4 V_R^{\mu l}}{64\pi^4} m_\mu m_l (C_0 + 2C_1) \int_0^1 dz \int_0^{1-z} dy \\ &\quad \times \frac{m_\mu^2 (1 - 2(y+z) + (y+z)^2) + M_N M_\nu}{zM_{N_l}^2 + yM_\nu^2 + (1-y-z)M_W^2 - (y+z)(1-y-z)m_\mu^2}. \end{aligned} \quad (21)$$

where the superscript SN stands for the sterile neutrino effects and the summation $l = e, \mu, \tau$ is over three lepton families. In the Appendix (A), we present more details of the calculation to achieve the result (19). The contributions of the Feynman diagrams (b) and (c) are obtained in a similar way.

The total sterile neutrino contribution on μ AMM is given by,

$$\Delta a_\mu^{SN} = \Delta a_\mu^{SN(a)} + \Delta a_\mu^{SN(b)} + \Delta a_\mu^{SN(c)}. \quad (22)$$

However, due to the smallness of the right-handed couplings \mathcal{G}_R , $SU_L(2)$ coupling g_w and active neutrino masses M_ν , the main contribution arises from $a_{(a)}^{SN}$. Keeping this point in mind and for the case that $M_N \ll M_W$, relation (19) will be reduced as follows

$$\Delta a_\mu^{SN(a)} = \frac{2\mathcal{G}_R^2 g_w^2 m_\mu^2}{(4\pi)^2 M_W^2} V_R^{\mu l} V_R^{\dagger \mu l} \left(\frac{7}{6} - \frac{5}{6} \left(\frac{M_N}{M_W} \right)^2 + \frac{1}{3} \left(\frac{m_\mu}{M_W} \right)^2 \right). \quad (23)$$

Based on this relation, one can decide what percentage of the μ anomaly can be compensated by this right-handed sterile neutrino interaction. It is due to the right-handed neutrino and left-handed lepton mixing introduced by the four-fermion introduction (11). In this regard, we have provided Fig. 5 in which the percentage of the μ anomaly compensation has been plotted in terms of \mathcal{G}_R . It should be mentioned that the density plot is confined between the upper and lower experimental values of Δa_μ^{SN} , $((2.49 \pm 48) \times 10^{-9})$, respectively. As it can be seen from the figure, the smaller values of the coupling constant will contribute less to the compensation of the muon

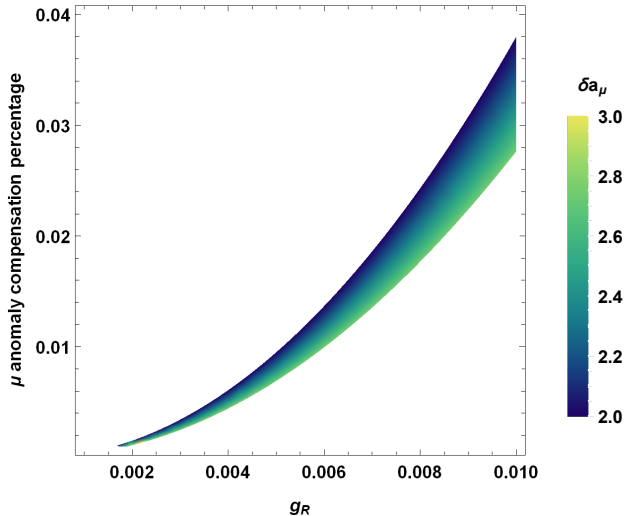


FIG. 5. The percentage of the $\Delta\mu$ anomaly compensation in terms of \mathcal{G}_R . Note: δa_μ stands for $\delta a_\mu = 10^9 \Delta a_\mu$

anomaly. For instance, the interaction of right-handed sterile neutrinos with coupling constant of the order of $\mathcal{G}_R \approx 0.004$ can account for less than 0.01% of the total anomaly.

Before ending this part, it is worth reviewing some results beyond the well-known $\alpha/2\pi$ term for the μ AMM from QED contribution. In this regard, the one-loop contributions to μ AMM due to the electroweak interactions of the SM were calculated quite a long time ago by Bardeen and et. al. [37]. They computed approximately 20 Feynman diagrams in the one-loop level and finally showed that the result is finite. The corresponding outcome was given by [38]

$$a_\mu^{\text{Weak}} = \frac{g_w^2 m_\mu^2}{64\pi^2 M_w^2} \left\{ \frac{10}{3} + \frac{4}{3}(v_\mu^2 - 5a_\mu^2) + \mathcal{O}\left(\frac{m_\mu^2}{M_Z^2} \log \frac{M_Z^2}{m_\mu^2}\right) + 2 \int_0^1 dx \frac{x^2(2-x)}{x^2 + \frac{M_H^2}{m_\mu^2}(1-x)} \right\} \quad (24)$$

Where v_μ and a_μ denote the vector and axial-vector couplings of the Z boson to the muon, respectively. Moreover, for a fermion f :

$$v_f = I_f^{(3)} - 2Q_f \sin^2 \theta_W, \quad a_f = I_f^{(3)}. \quad (25)$$

It is important to note that Eq. (24) contains extra terms that are divergent and arise from the anomaly that results when the triangle is multiplied by k_μ . However, this anomaly vanishes and the result becomes finite and gauge invariant if one sums over a complete fermion's generation and considers all of the Feynman diagrams [38].

Moreover, Bardeen and Lautrup used the approach of dimensional regularization in [37] and obtained the contribution of W boson interacting with left-handed active neutrinos ν_L , being the

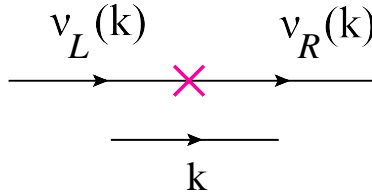
counterpart of the Feynman diagram (a) of Fig.(4), as follows

$$a_{\mu}^{\nu} \simeq -\frac{1}{64\pi^2} \frac{g_w^2 m_{\mu}^2}{M_w^2} \frac{10}{3} = -9.11 \times 10^{-11}, \quad (26)$$

where m_{μ} is the muon mass and the active neutrino mass is set to zero. We followed the same approach to calculate the contribution of Fig.(4a) for W boson interacting with the right-handed sterile neutrinos ν_R^{ℓ} in three generations. Compared with the corresponding calculations in SM, the differences come from the right-handed coupling $\mathcal{G}_R g_w$, sterile neutrino masses $M_{N_l} \gg M_{\nu_l}$ and right-handed family mixing matrix $V_R^{\mu l}$ instead of PMNS mixing matrix $V_L^{\mu l}$. In addition, as it is expected, $a_{(a)}^{SN}$ reduces to a_{μ}^{ν} (26) when $\mathcal{G}_R^2 \rightarrow 1$, $M_{N_l} \rightarrow 0$ and $\sum_l V_R^{\mu l} V_R^{\dagger \mu l} = 1$.

B. Contribution due to W boson mediation with Left-Right neutrino mixing: Non-standard neutrino interactions

In this part, we consider another possibility of the right handed sterile neutrino contribution to μ AMM which has been depicted in Fig.6. Indeed, due to the mass of the neutrino, the helicity flip may occur in the mediator part, producing an exotic coupling, which is often referred to as *non-standard neutrino interactions*. This process is similar to those that happen for the Weinberg operator, introduced to explain $0\nu\beta\beta$ [62]. Based on this method, we treat the mass terms in Eq. (12) as a 'two-point vertex'. By considering the neutrino as a Dirac particle, M_N is the Dirac neutrino mass matrix connecting one massless left-handed neutrino of momentum k with the right-handed one of the same momentum. Analogously to the Weinberg operator studied in Fig. 1 and Eq. 6 of Ref. [63], its graph simplifies to:



By associating left-handed neutrino coupling vertex $g_w P_L \gamma^\nu$ to W gauge boson and right-handed neutrino coupling vertex $\mathcal{G}_R g_w P_L \gamma^\rho$ to W gauge boson to we have

$$\mathcal{G}_R g_W^2 (V_L^{\mu l})^\dagger \gamma^\nu P_R \frac{iM_D^l}{k^2} P_R \gamma^\rho V_R^{\mu l}, \quad (27)$$

in the Feynman diagram 6. where l family flavors are summed, and we will approximately select the large M_D value.

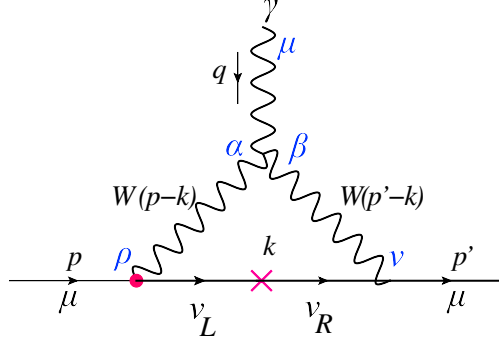


FIG. 6. Feynman diagram related to the helicity flip of neutrino mediator. The red cross (\times) represents non-standard neutrino interactions, i.e., the Dirac mass insertion.

From this perspective and making use of (12) and (13), the vertex correction due to this diagram will be obtained as follows

$$\begin{aligned}
\bar{u}(p')(-ie\Gamma^\mu)u(p) &= -ieV_L^{\mu l}V_R^{\dagger\mu l}\int\frac{d^4k}{(2\pi)^4}\left\{\bar{u}(p')\left(\frac{-i\mathcal{G}_Rg_w}{2\sqrt{2}}\right)\gamma^\nu(1+\gamma_5)\frac{iM_D^l}{k^2}\left(\frac{-ig_w}{2\sqrt{2}}\right)\gamma^\rho(1-\gamma_5)\right. \\
&\times u(p)\frac{-i}{(p-k)^2-M_W^2}\frac{-i}{(p'-k)^2-M_W^2}\left[g_{\rho\alpha}-\frac{(p-k)_\rho(p-k)_\alpha}{M_W^2}\right] \\
&\times\left[g_{\nu\beta}-\frac{(p'-k)_\nu(p'-k)_\beta}{M_W^2}\right]\left[g^{\beta\alpha}(2k-p-p')^\mu\right. \\
&\left.+g^{\alpha\mu}(2p-p'-k)^\beta+g^{\mu\beta}(2p'-k-p)^\alpha\right]\left.\right\}. \tag{28}
\end{aligned}$$

Then taking steps similar to that explained in Appendix A, we get the following correction on the a_μ due to the mentioned diagram of Fig. (6)

$$\begin{aligned}
\Delta a_\mu^{SN(\times)} &= \left(\frac{\mathcal{G}_Rg_w^2}{64\pi^2}\right)V_L^{\mu l}V_R^{\dagger\mu l}m_\mu M_D\int_0^1dz\int_0^{1-z}dy \\
&\times\frac{6z}{(y+z)M_W^2-(y+z)(1-y-z)m_\mu^2+1-y-z}. \tag{29}
\end{aligned}$$

where we have assumed that the intermediate neutrino is a Dirac particle. Performing the above integral, we come to the conclusion that

$$\begin{aligned}
\Delta a_\mu^{SN(\times)} &= \left(\frac{3\mathcal{G}_Rg_w^2}{64\pi^2}\right)\frac{m_\mu M_D}{M_W^2}V_L^{\mu l}V_R^{\dagger\mu l} \\
&= \frac{3\mathcal{G}_R}{16\sqrt{2}\pi^2}G_F m_\mu M_D V_L^{\mu l} V_R^{\dagger\mu l}. \tag{30}
\end{aligned}$$

Now, we can use this result to set constraints on \mathcal{G}_R . By rewriting the above relation as below

$$\Delta a_\mu^{SN(\times)} \approx 10^{-6}\mathcal{G}_R, \quad \left(\frac{m_\mu}{105MeV}\right)\left(\frac{M_D}{100GeV}\right)\left(\frac{G_F}{1.05\times 10^{-5}GeV^{-2}}\right) \tag{31}$$

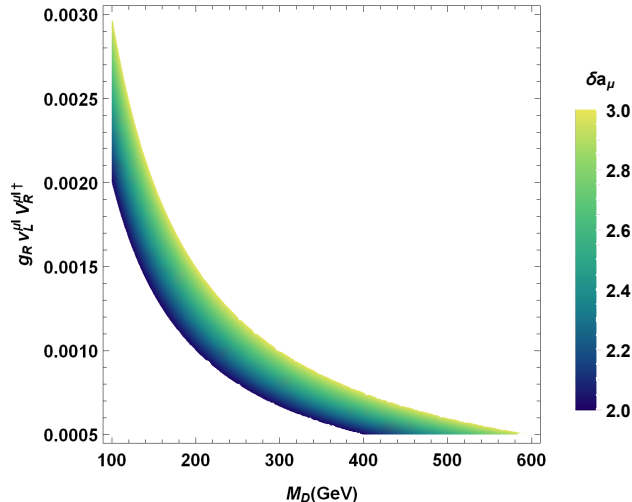


FIG. 7. Allowed parameter space in agreement with the μ AMM. Note: δa_μ stands for $\delta a_\mu = 10^9 \Delta a_\mu$

and employing the fact that $\Delta a_\mu = (2.49 \pm 0.48) \times 10^{-9}$, we get the result that $\mathcal{G}_R < 10^{-3}$ for $M_D \approx 100 \text{ GeV}$. However, for $M_D \ll 100 \text{ GeV}$ and $\mathcal{G}_R < 10^{-3}$ case, the contribution $\Delta a_\mu^{SN(\times)}$ to the μ AMM should be too small to account for the muon anomaly Δa_μ .

To gain a clearer understanding of our results, we have plotted Fig.(7) which shows the Δa_μ^{SN} dependence on the effective coupling $\mathcal{G}_R, V_L^{\mu l} V_R^{\mu l \dagger}$ and the Dirac mass scale M_D . The density plot is confined between the upper and lower experimental values $(249(48) \times 10^{-11})$, respectively, of Δa_μ^{SN} within 5σ CL. The plot represents the allowed region of the model parameters that satisfy the experimental data on Δa_μ^{SN} and can explain the current deviation between the experimental measurement and the theoretical prediction.

In addition, the contribution arising from this sort of right-handed sterile neutrino interaction with SM particle to Δa_μ , for $M_D \approx 100 \text{ GeV}$, is presented in Fig. 8 (left panel). As it is clear from this figure, for the \mathcal{G}_R coupling constant around 0.002, this type of right-handed neutrino interaction can address the whole anomaly and play a significant role in the context of μ AMM. Moreover, to be more clear, we have provided the percentage of the μ anomaly compensation in terms of \mathcal{G}_R in the right panel of Fig. 8.

Before ending this part, it is necessary to mention that one of the most famous possibilities to explain very light neutrino masses is the type-I seesaw mechanism through which SM neutrinos acquire tiny Majorana masses. However, the type-I seesaw model suffers from a lack of testability, because right-handed neutrinos are too heavy to be produced in current collider experiments (For a Dirac mass $M_D \sim 100 \text{ GeV}$, it requires a Majorana mass $M_M \gtrsim 10^{12} \text{ GeV}$ to achieve SM neutrino masses $\lesssim 1 \text{ eV}$). To overcome this problem, several models have been proposed that can

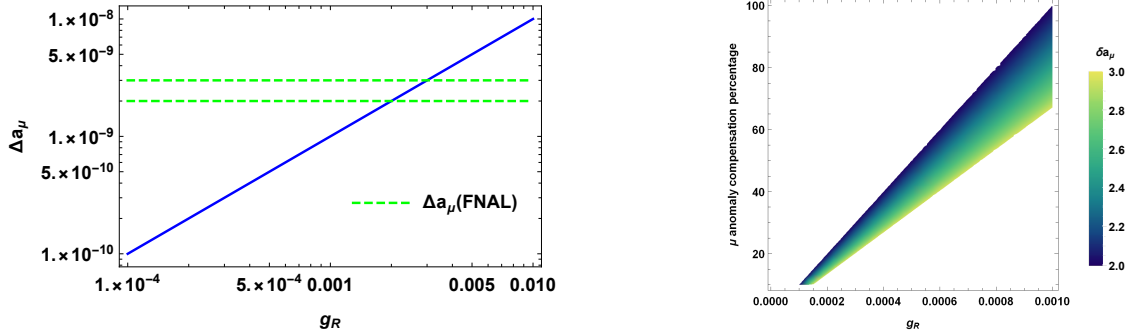


FIG. 8. Left: The contribution due to the right-handed sterile neutrino interaction with SM particle to Δa_μ versus \mathcal{G}_R for $M_D \approx M_W$. Right: The percentage of the μ anomaly compensation in terms of \mathcal{G}_R . Note: δa_μ stands for $\delta a_\mu = 10^9 \Delta a_\mu$. In addition, the density plot is confined between the upper and lower experimental values of Δa_μ^{SN} $((2.49 \pm 0.48) \times 10^{-9})$, respectively.

lead to sub-eV neutrino masses while keeping heavy Majorana neutrino masses as low as several hundred GeV [64–66]. Particularly, authors in [67] have shown that implementing an additional U(1) symmetry and then its soft breaking can veer into having Majorana masses at the order of TeVs. These issues will be topics for our future investigations.

V. SUMMARY AND REMARKS

Recent experimental measurements on μ AMM represent considerable discrepancies with SM predictions. These differences might be understood in scenarios of physics beyond SM with new particles and interactions. In this work, we investigated the right-handed sterile neutrino contributions to the $(g - 2)_\mu$ anomaly within an effective four-fermion interacting model based on the fundamental symmetries and particle content of the SM. To this end, we first calculated the magnetic dipole form factor (F_2) for the muon particle by considering the standard sterile neutrino interaction which is the interaction including W boson and ν_R mediation. Making use of the effective 1PI operators (13) and (15) and obtaining the correction effects on the μ AMM due to the interaction between the right-handed sterile neutrino and the SM particles through the Feynman diagrams depicted in Fig (4), we found that these kinds of standard neutrino interactions cannot account for the muon $g - 2$ anomaly, because as one can see in (23), the corrections are proportional to m_μ^2/M_W^2 , similar to SM corrections. This should be avoided by a mechanism of chiral enhancement [68, 69]. Indeed, we obtain the promising correction (30), which is proportional to $m_\mu M_D/M_W^2$, originating from the chirality flipping a large Dirac mass M_D of sterile neutrinos.

Next, we considered the non-standard Dirac neutrino interactions being due to W boson me-

diation with Left-Right neutrino mixing, illustrated via the Feynman diagram in Fig (6). As our studies showed, if neutrinos can experience such an exotic coupling, they will play an important role in explaining $(g - 2)_\mu$ anomaly. In continuation, we tried to analyze the implications of our results in the μ AMM and to study the constraint on the parameter space of right-handed sterile neutrino using the experimental data of a_μ , which the discussions are as follows:

- Making use of the obtained correction term on the a_μ , i.e. Eq. (29), we found that a Dirac mass scale M_D around the 100 GeV could explain the muon anomaly if the right handed sterile neutrino's coupling with SM particles is about $\mathcal{G}_R \approx 10^{-3}$. If the Dirac mass scale is much smaller than 100 GeV, the sterile neutrino contributions to the μ AMM are too small to explain the muon anomaly.
- Using the obtained correction term on the a_μ , i.e. Eq.(30), we plotted the Δa_μ^{SN} dependence on the effective coupling effective coupling $\mathcal{G}_R, V_L^{\mu l} V_R^{\dagger \mu l}$ and the Dirac mass scale M_D in Fig.(7). This plot represents the allowed region of the model parameters that satisfy the experimental data on Δa_μ^{SN} and can explain the current deviation between the experimental measurement and the theoretical prediction.
- In addition, we provided Fig. (8) (left panel) for presenting the contribution to Δa_μ due to this sort of right-handed sterile neutrino interaction with SM particle. In the right panel of Fig. (8), the percentage of the μ anomaly compensation in terms of \mathcal{G}_R has been plotted. According to this figure, for the $\mathcal{G}_R \approx 0.002$ and $M_D \approx 100\text{GeV}$, the right-handed neutrino can address the whole anomaly and play a significant role in the context of μ AMM.

To further constrain sterile neutrinos' effective mass scale and coupling to SM particles, we necessarily require more experiments and observations.

Before ending this paper it should be mentioned that the impacts of the effective operators and Feynman diagrams on processes involving different lepton flavors, and explore the constraints by using lepton flavor-violating observables will be investigated in an independent work [70].

ACKNOWLEDGMENT

I. Motie would like to express his gratitude to Professor A. Blanchard for his gracious hospitality during my stay in Toulouse, France. S. S. Xue thanks Drs S. Shakeri and F. Hajkarim for discussions. S. Mahmoudi is grateful to the Iran Science Elites Federation for the financial support.

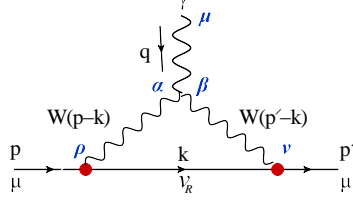


FIG. 9. One of the Feynman diagrams which gives the W-boson contribution to the muon anomalous moment.

Appendix A: Appendix

In order to evaluate loop integrals that come from Feynman diagrams, we need to use the Feynman parametrization technique together with the Dirac equation and the standard contraction identity of gamma matrices. For a more in-depth understanding of this method, please see [71].

In the context of Quantum Field Theory (QFT), the computation of vertex corrections of photon-fermion has a unique procedure that can be found in QFT textbooks (e.g. see the chapter 6 of [71]).

In loop integrals, we often encounter products of many propagator factors. To simplify the process of four-momentum integration, we can combine these propagators into a single fraction. This is commonly done using what are known as Feynman parameters [71].

Here, we provide additional details for Feynman diagram (4-a). For other diagrams, everything remains the same. Considering Eq. (13) and Fig. (9), the vertex correction will be as follows

$$\begin{aligned}
\bar{u}(p') \left(-ie\Gamma_{(a)}^\mu \right) u(p) &= -ie V_R^{\mu l} V_R^{\dagger \mu l} \int \frac{d^4 k}{(2\pi)^4} \\
&\times \left\{ \bar{u}(p') \left(\frac{-i\mathcal{G}_R g_w}{\sqrt{2}} \right) \gamma^\nu (1 + \gamma_5) \frac{i}{\not{k} - M_{N_l}} \left(\frac{-i\mathcal{G}_R g_w}{\sqrt{2}} \right) \gamma^\rho (1 + \gamma_5) \right. \\
&\times u(p) \frac{-i}{(p-k)^2 - M_W^2} \frac{-i}{(p'-k)^2 - M_W^2} \left[g_{\rho\alpha} - \frac{(p-k)_\rho (p-k)_\alpha}{M_W^2} \right] \\
&\times \left[g_{\nu\beta} - \frac{(p'-k)_\nu (p'-k)_\beta}{M_W^2} \right] \left[g^{\beta\alpha} (2k - p - p')^\mu \right. \\
&\left. \left. + g^{\alpha\mu} (2p - p' - k)^\beta + g^{\mu\beta} (2p' - k - p)^\alpha \right] \right\}. \tag{A1}
\end{aligned}$$

To evaluate the above integral, we first use the Feynman parameters' method [71] to squeeze the three denominator factors into a single quadratic polynomial, raised to the third power, as follows

$$\frac{1}{[k^2 - M_{N_l}^2 + i\epsilon] [(p'-k)^2 - M_W^2 + i\epsilon] [(p-k)^2 - M_W^2 + i\epsilon]} = \int_0^1 dx dy dz \delta(x+y+z-1) \frac{2}{D^3} \tag{A2}$$

where the variable x , y and z are called Feynman parameters and the new variable D is defined is

given by

$$\begin{aligned} D &= x[k^2 - M_{N_i}^2] + y[(p' - k)^2 - M_W^2] + z[(p - k)^2 - M_W^2] \\ &= k^2 - 2k \cdot (yp' + zp) - M_w^2(y + z) - x M_{N_i}^2 + m^2(y + z) + i\epsilon, \end{aligned} \quad (\text{A3})$$

where in the second line we have used $x + y + z = 1$. Now, one can shift k to complete the square

$$l \equiv k - (yp' + zp), \quad (\text{A4})$$

and after a bit of calculation, we find that D simplifies to

$$D = l^2 - \Delta_{(a)} + i\epsilon, \quad (\text{A5})$$

where

$$\Delta_{(a)} = -x(1-x)m^2 + (1-x)M_W^2 + xM_{N_i}^2 - z y q^2. \quad (\text{A6})$$

In the next step, we must express the numerator of (A1), i.e.

$$\begin{aligned} \text{Numerator} &= \bar{u}(p')\gamma^\nu(1+\gamma_5)(\not{k} + M_{N_i})\gamma^\rho(1+\gamma_5)\left[g_{\rho\alpha} - \frac{(p-k)_\rho(p-k)_\alpha}{M_W^2}\right] \\ &\times \left[g_{\nu\beta} - \frac{(p'-k)_\nu(p'-k)_\beta}{M_W^2}\right] [g^{\beta\alpha}(2k-p-p')^\mu \\ &+ g^{\alpha\mu}(2p-p'-k)^\beta + g^{\mu\beta}(2p'-k-p)^\alpha] u(p), \end{aligned} \quad (\text{A7})$$

in terms of l . Making use of the following identities

$$\begin{aligned} \int \frac{d^4 l}{(2\pi)^4} \frac{l^\mu}{D^3} &= 0, \\ \int \frac{d^4 l}{(2\pi)^4} \frac{l^\mu l^\nu}{D^3} &= \int \frac{d^4 l}{(2\pi)^4} \frac{g^{\mu\nu} l^2}{4 D^3} \end{aligned} \quad (\text{A8})$$

and considering the terms with the highest order, the numerator changes into

$$\begin{aligned} \text{Numerator} &\rightarrow \bar{u}(p') \left\{ \gamma^\mu(1+\gamma_5) \left[-3l^2 + \left(z(1-2z) + y(1-2y) + 2z(2-y) + 2y(2-z) \right) m^2 \right. \right. \\ &\quad \left. \left. - \left(y(2-z) - z(2-y) \right) q^2 \right] (1+\gamma_5) \left[(-2y-2z-4yz)mp^\mu - 2y(2y-1)mp'^\mu \right] \right. \\ &\quad \left. + (1-\gamma_5) \left[(-2y-2z-4yz)mp'^\mu - 2z(2z-1)mp^\mu \right] \right. \\ &\quad \left. + \gamma^\mu(1-\gamma_5) \left(-2zy + y + 3z \right) m^2 \right\} u(p) \end{aligned} \quad (\text{A9})$$

Henceforth, we just interested in the terms contributing to the μ AMM. By employing (10) as well as the Gordon Identity

$$\bar{u}(p')\gamma^\mu u(p) = \bar{u}(p')\left(\frac{(p+p')^\mu}{2m} + i\frac{\sigma^{\mu\nu}q_\nu}{2m}\right)u(p), \quad (\text{A10})$$

one can find that the terms that contribute to the magnetic moment are those that are multiplied by $\frac{(p+p')^\mu}{2m}$. Therefore, the correction on the μ AMM will be obtained as follows

$$\begin{aligned} \delta\Gamma_{(a)}^\mu &= -i(\mathcal{G}_R g_w)^2 V_R^{\mu l} V_R^{\dagger\mu l} \int \frac{d^4 l}{(2\pi)^4} \int_0^1 dx dy dz \delta(x+y+z-1) \frac{2}{(l^2 - \Delta_{(a)})^3} \\ &\quad \left((-2y - 4yz - 4z^2)mp^\mu + (-2z - 4yz - 4y^2)mp'^\mu \right). \end{aligned} \quad (\text{A11})$$

To go further and evaluate the above integral, we use the following relation

$$\int \frac{d^4 l}{(2\pi)^4} \frac{1}{(l^2 - \Delta)^n} = \frac{(-1)^n i \Gamma(n-2)}{(4\pi)^2} \frac{1}{\Gamma(n)} \left(\frac{1}{\Delta}\right)^{n-2}, \quad (\text{A12})$$

and we get

$$\delta\Gamma_{(a)}^\mu = -\left(\frac{\mathcal{G}_R g_w}{4\pi}\right)^2 V_R^{\mu l} V_R^{\dagger\mu l} \int_0^1 dx dy dz \delta(x+y+z-1) \frac{1}{\Delta_{(a)}} (-2y - 4yz - 4z^2)(p^\mu + p'^\mu) m. \quad (\text{A13})$$

Using the above result, we conclude that the correction on the μ AMM due to the participation of the Sterile Neutrino at the zero momentum transfer is as follows

$$\begin{aligned} a_{(a)}^{SN} &= -2\left(\frac{\mathcal{G}_R g_w}{4\pi}\right)^2 m_\mu^2 V_R^{\mu l} V_R^{\dagger\mu l} \int_0^1 dz \int_0^{1-z} dy \\ &\quad \times \frac{-2y - 4yz - 4z^2}{M_W^2(y+z) + (1-y-z)M_{N_i}^2 - (y+z)(1-y-z)m_\mu^2}. \end{aligned} \quad (\text{A14})$$

Note that we adopted the γ_5 anti-commutes with all γ matrices. Eqs. (16), (17) and (18) contain a common part, which is divergent and arises from the anomaly that results when the triangle is multiplied by k_μ . The anomaly vanishes and the result becomes finite and gauge invariant only when one sums over a complete generation, as discussed in Ref. [37, 38].

-
- [1] A. M. Green, SciPost Phys. Lect. Notes **37**, 1 (2022)
 - [2] L. Roszkowski, Pramana **62**, 389-401 (2004)
 - [3] Q. R. Ahmad *et al.* [SNO], Phys. Rev. Lett. **89**, 011302 (2002)
 - [4] L. Canetti, M. Drewes and M. Shaposhnikov, New J. Phys. **14**, 095012 (2012)
 - [5] D. P. Aguillard *et al.* [Muon g-2], Phys. Rev. Lett. **131**, no.16, 161802 (2023)
 - [6] G. W. Bennett *et al.* [Muon g-2], Phys. Rev. D **73**, 072003 (2006)

- [7] T. Aoyama, N. Asmussen, M. Benayoun, J. Bijnens, T. Blum, M. Bruno, I. Caprini, C. M. Carloni Calame, M. Cè and G. Colangelo, *et al.* Phys. Rept. **887**, 1-166 (2020)
- [8] S. Borsanyi, Z. Fodor, J. N. Guenther, C. Hoelbling, S. D. Katz, L. Lellouch, T. Lippert, K. Miura, L. Parato and K. K. Szabo, *et al.* Nature **593**, no.7857, 51-55 (2021)
- [9] D. Borah, M. Dutta, S. Mahapatra and N. Sahu, Phys. Lett. B **820**, 136577 (2021)
- [10] L. Zu, X. Pan, L. Feng, Q. Yuan and Y. Z. Fan, JCAP **08**, no.08, 028 (2022)
- [11] P. Athron, C. Balázs, D. H. J. Jacob, W. Kotlarski, D. Stöckinger and H. Stöckinger-Kim, JHEP **09**, 080 (2021)
- [12] A. Keshavarzi, K. S. Khaw and T. Yoshioka, Nucl. Phys. B **975**, 115675 (2022)
- [13] M. Lindner, M. Platscher and F. S. Queiroz, Phys. Rept. **731**, 1-82 (2018)
- [14] J. Cao, J. Lian, Y. Pan, D. Zhang and P. Zhu, JHEP **09**, 175 (2021)
- [15] A. Hammad, A. Rashed and S. Moretti, Phys. Lett. B **827**, 136945 (2022)
- [16] S. Aghababaei, M. Haghghat and I. Motie, Phys. Rev. D **96**, 115028 (2017)
- [17] A. Dey, J. Lahiri and B. Mukhopadhyaya, Phys. Rev. D **106**, no.5, 055023 (2022)
- [18] M. Chakraborti, S. Heinemeyer and I. Saha, Eur. Phys. J. C **80**, no.10, 984 (2020)
- [19] J. S. Alvarado, S. F. Mantilla, R. Martinez, F. Ochoa and C. Sierra, Phys. Rev. D **108**, no.9, 095040 (2023)
- [20] K. Ghorbani, Phys. Rev. D **104**, no.11, 115008 (2021)
- [21] L. A. Anchordoqui, I. Antoniadis, X. Huang, D. Lust and T. R. Taylor, Fortsch. Phys. **69**, no.8-9, 2100084 (2021)
- [22] S. Zhou, Chin. Phys. C **46**, no.1, 011001 (2022)
- [23] C. T. Lu, R. Ramos and Y. L. S. Tsai, JHEP **08**, 073 (2021)
- [24] O. M. Boyarkin, G. G. Boyarkina and V. V. Makhnach, Phys. Rev. D **77**, 033004 (2008)
- [25] C. Majumdar, S. Patra, P. Pritimita, S. Senapati and U. A. Yajnik, JHEP **09**, 010 (2020)
- [26] D. N. Dinh, Nucl. Phys. B **994**, 116306 (2023)
- [27] W. Abdallah, A. Awad, S. Khalil and H. Okada, Eur. Phys. J. C **72**, 2108 (2012)
- [28] S. S. Xue, JHEP **05**, 146 (2017)
- [29] S. S. Xue, JHEP **11**, 072 (2016)
- [30] S. S. Xue, JHEP **05**, 146 (2017)
- [31] T. Burnett and M. J. Levine, Phys. Lett. B **24**, 467-468 (1967)
- [32] P. Stoffer, G. Colangelo and M. Hoferichter, JINST **18**, no.10, C10021 (2023)
- [33] B. E. Lautrup and E. De Rafael, Phys. Rev. **174**, 1835-1842 (1968)
- [34] J. Aldins, T. Kinoshita, S. J. Brodsky and A. J. Dufner, Phys. Rev. D **1**, 2378 (1970)
- [35] B. E. Lautrup, Phys. Lett. B **38**, 408-410 (1972)
- [36] G. Auberson and Ling-Fong Li. Phys. Rev. D **5**, 2269 (1972)
- [37] W. A. Bardeen, R. Gastmans and B. E. Lautrup, Nucl. Phys. B **46**, 319-331 (1972)
- [38] S. Peris, M. Perrottet and E. de Rafael, Phys. Lett. B **355**, 523-530 (1995)

- [39] J. S. Schwinger, Phys. Rev. **73**, 416-417 (1948)
- [40] P. Kusch and H. M. Foley, Phys. Rev. **74**, no.3, 250 (1948)
- [41] K. Abazajian, G. M. Fuller and M. Patel, Phys. Rev. D **64**, 023501 (2001)
- [42] K. N. Abazajian, Phys. Rept. **711-712**, 1-28 (2017)
- [43] M. Drewes, T. Lasserre, A. Merle, S. Mertens, R. Adhikari, M. Agostini, N. A. Ky, T. Araki, M. Archidiacono and M. Bahr, *et al.* JCAP **01**, 025 (2017)
- [44] A. A. Aguilar-Arevalo *et al.* [MiniBooNE], Phys. Rev. Lett. **129**, no.20, 201801 (2022)
- [45] A. Boyarsky, M. Drewes, T. Lasserre, S. Mertens and O. Ruchayskiy, Prog. Part. Nucl. Phys. **104**, 1-45 (2019)
- [46] M. Ibe, A. Kusenko and T. T. Yanagida, Phys. Lett. B **758**, 365-369 (2016)
- [47] H. B. Nielsen and M. Ninomiya, Nucl. Phys. B **193**, 173-194 (1981)
- [48] H. B. Nielsen and M. Ninomiya, Phys. Lett. B **105**, 219-223 (1981)
- [49] S. S. Xue, Nucl. Phys. B **990**, 116168 (2023)
- [50] S. S. Xue, Nucl. Phys. B **980**, 115817 (2022)
- [51] S. S. Xue, Phys. Rev. D **93**, no.7, 073001 (2016)
- [52] A. Tumasyan *et al.* [CMS], Phys. Rev. Lett. **131**, no.1, 011803 (2023)
- [53] A. M. Sirunyan *et al.* [CMS], Phys. Rev. Lett. **120**, no.22, 221801 (2018)
- [54] A. M. Sirunyan *et al.* [CMS], JHEP **01**, 122 (2019)
- [55] S. S. Xue, Phys. Rev. D **93**, no.7, 073001 (2016)
- [56] L. Pacioselli, O. Panella, M. Presilla and S. S. Xue, JHEP **11**, 054 (2023)
- [57] M. Haghghat, S. Mahmoudi, R. Mohammadi, S. Tizchang and S. S. Xue, Phys. Rev. D **101**, no.12, 123016 (2020)
- [58] S. S. Xue, Nucl. Phys. B **985**, 115992 (2022)
- [59] S. Mahmoudi, M. Sadegh, J. Khodagholizadeh, I. Motie, S. S. Xue and A. Blanchard, Eur. Phys. J. C **84**, no.6, 619 (2024)
- [60] S. Shakeri, F. Hajkarim and S. S. Xue, JHEP **12**, 194 (2020)
- [61] G. Passarino and M. J. G. Veltman, Nucl. Phys. B **160**, 151-207 (1979)
- [62] S. Weinberg, Phys. Rev. Lett. **43**, 1566-1570 (1979)
- [63] B. Fuks, J. Neundorff, K. Peters, R. Ruiz and M. Saimpert, Phys. Rev. D **103**, no.11, 115014 (2021)
- [64] A. Pilaftsis, Z. Phys. C **55**, 275-282 (1992)
- [65] J. Kersten and A. Y. Smirnov, Phys. Rev. D **76**, 073005 (2007)
- [66] R. N. Mohapatra and J. W. F. Valle, Phys. Rev. D **34**, 1642 (1986)
- [67] H. Zhang and S. Zhou, Phys. Lett. B **685**, 297-301 (2010)
- [68] A. Crivellin and M. Hoferichter, JHEP **07**, 135 (2021) [erratum: JHEP **10**, 030 (2022)]
- [69] A. Crivellin, M. Hoferichter and P. Schmidt-Wellenburg, Phys. Rev. D **98**, no.11, 113002 (2018)
- [70] I. Motie, S. Mahmoudi and S.-S. Xue, muon- electron conversion and sterile neutrino , in preparation.
- [71] Michael Edward Peskin and Daniel V. Schroeder. An Introduction to Quantum Field Theory. Reading,

USA: Addison-Wesley (1995) 842 p. Westview Press, 1995.

